J Eng Math (2017) 104:19–39
DOI 10.1007/s10665-016-9870-x

The steady-state response of size-dependent functionally graded nanobeams to subharmonic excitation

S. Ziaee

Received: 6 September 2015 / Accepted: 20 July 2016 / Published online: 5 August 2016

Abstract This study aims to investigate the nonlinear forced vibration of functionally graded (FG) nanobeams. It is assumed that material properties are gradually graded in the direction of thickness. Nonlocal nonlinear Euler–Bernoulli beam theory is used to derive nonlocal governing equations of motion. The linear eigenmodes of FG nanobeams are used to transform a partial differential equation of motion into a system of ordinary differential equations via the Galerkin method. The multiple scale method is used to find the governing equations of the steady-state responses of FG nanobeams excited by a distributed harmonic force with constant intensity. It is also assumed that the working frequency is close to three times greater than the lowest natural frequency. Based on the equation governing the linear natural frequencies of FG nanobeams, the influence of the small scale parameter, material composition, and stiffness of the foundation on the linear relationship among natural frequencies is studied. Results show that superharmonic response or a combination of resonances may occur as well as a subharmonic response depending on the power-law index and stiffness of the foundation. Then the governing equations of a steady-state response of FG nanobeams for four possible solutions are obtained depending on the value of the small scale parameter. It is shown that the simplest response of FG nanobeams is a subharmonic response or superharmonic response. The equations governing the frequency–response curves are obtained and the effects of the power-law index and small scale parameter on them are discussed.

Keywords Euler–Bernoulli beam theory · FG nanobeam · Multiple scale method · Nonlocal nonlinear · Subharmonic response

1 Introduction

Functionally graded materials (FGMs) are advanced composite materials in which material properties change continuously and smoothly over a certain direction from one material to another. Because of gradual changes in material properties, not only is stress distribution in FGMs improved, but FGMs also exhibit higher fracture toughness and enhanced thermal resistance [1]. These unique characteristics of FGMs have made them exceptional materials that can be used in many engineering application fields [2], such as micro/nanoelectromechanical systems

S. Ziaee (✉)
Yasouj University, Yasouj, Iran
e-mail: ziaee@yu.ac.ir; sima_ziaee@yahoo.com

[3]. Therefore, the study of the mechanical behavior of FG micro-/nanostructures has been highly regarded by researchers recently.

It is well known that classical continuum theories are not able to correctly predict the mechanical behavior of micro- or nanoscale devices because they do not take the size effect into account. To incorporate the size effect into continuum mechanics, higher-order continuum theories that contain additional material constants have been developed [4,5]. Strain gradient theory [6–8], modified strain gradient theory [7], couple stress theory [8], and modified couple stress theory [6,7,9,10] are some of the well-known higher-order theories used to incorporate the size effect into classical continuum theories.

Among the higher-order theories whose constitutive equations contain one new length scale as well as Lame constants, Eringen nonlocal elasticity is widely used to simulate static and instability behavior [3,11,12], linear free vibration [13–17], linear forced vibration [18], and nonlinear free vibration [19,20] of functionally graded (FG) nanobeams. The effect of in-plane thermal loading on the vibrational behavior of FG nanobeams has also been studied via nonlocal beam theories [21–24].

Eringen's theory relates to integral-type nonlocalities, where volume averages of state variables are computed [5], although Eringen formulated another theory of nonlocal elasticity in which the integrals are replaced by gradients. In the earlier theory, there is only one length-scale parameter (e_0a), including a material constant and internal characteristic length, and the constitutive equation of this theory is expressed based on the nonlocal stress tensor and Laplacian stress tensor [5].

It is abundantly clear that the selection of proper values of the nonlocal parameter guarantees the accuracy of the mechanical response simulation of micro-/nanostructures. Researchers who have studied the mechanical behavior of carbon nanostructures via both nonlocal continuum elasticity and the molecular dynamics method have shown that the value of the small scale parameter depends not only on the material but also on the boundary condition, chirality, aspect ratio, and the nature of the motion [19,25–33]. Zhang et al. [25] found a value of 0.82 nm for a nonlocal parameter when they compared the vibrational results of simply supported single-walled carbon nanotubes with molecular dynamics simulations. Based on a similar method, Hu et al. [26] reported nonlocal parameter values of 0.6 nm for the dispersion of transverse waves and 0.2–0.23 nm for the dispersion of torsional waves. Khademolhosseini et al. [27] presented nonlocal parameters of 0.85–0.86 nm for torsional buckling of armchair and zigzag single-walled carbon nanotubes. Ansari et al. [28] showed that the values of nonlocal parameters for axial buckling of single-walled carbon nanotubes change with the boundary conditions. They obtained nonlocal parameter values of 0.54 nm for simply supported boundary conditions, 0.531 nm for clamped–clamped boundary conditions, 0.55 nm for clamped–simply supported boundary conditions, and 0.722 nm for clamped–free boundary conditions [28]. Duan et al. [29] used molecular dynamic simulation results to estimate small scale parameters in nonlocal Timoshenko beam theory used to predict the natural frequencies of fully clamped and cantilever single-layered carbon nanotubes with different length/diameter ratios (L/d). Their results clearly show the significant effect of the boundary condition, aspect ratio, and mode shape on the value of small scale parameters. They reported that the small scale value can vary from 0 to 2.66 nm. The small scale parameters proposed by Ansari et al. [30] to model the lateral vibration of single graphene sheets are completely dependent on boundary conditions (1.41 and 0.87 nm for simply supported and fully fixed zigzag graphene sheets, respectively), are slightly affected by chirality (1.34 and 0.71 nm for simply supported and fully fixed armchair graphene sheets, respectively), and are independent of the nanoplate size, while Shen et al.'s study [31] shows that the size of the nanoplate as well as chirality impact the small scale parameter. Their results demonstrate that the small scale value varies from 0.22 to 0.67 nm for single-layer graphene sheets because of the different values of the aspect ratio and different chiral angles [31]. Ansari and Sahmani [32] predicted the appropriate value of nonlocal parameters to simulate the biaxial buckling of single-layer graphene sheets. Their results clearly reveal that, in contrast to the type of nonlocal plate used to simulate the biaxial buckling of a graphene sheet that can impact the value of the small scale parameter, chirality is not a parameter that affect the small scale value [32]. Miandoab et al. [33] estimated the nonlocal parameter value to be 8 μm to study the vibration of polysilicon microbeams.

On the other hand, Peddieson et al.'s study [34] on micro-/nanocantilever actuators reveals that the magnitude of the beam length can change the importance of the small scale parameter in the prediction of mechanical responses

of micro-/nanostructures. They demonstrated that, in contrast to nanoscale devices, microscale devices might not exhibit nonlocal effects [34]. Nevertheless, a thorough study has not yet been undertaken to estimate the value of the small scale parameter corresponding to mechanical response of FG micro-/nanobeams [19].

Based on the author's knowledge, there are no experimental studies or molecular simulations of the mechanical behavior of FG nanostructures to clarify how to use the small scale parameter in the governing equations of FG nanostructures. Whether the small scale parameter must be gradually graded through the volume as is done for other material properties or whether it can be used as a corrective factor of classical theory is a question that remains unanswered. It must be noted that, contrary to other mechanical properties, the value of small scale parameter not only depends on the material but also varies according to the boundary conditions and the nature of the motion. It is also worth mentioning that Shen et al. [35] used a single value of small scale parameter when they studied the nonlinear vibration of bilayered graphene sheets composed of armchair and zigzag layers by matching nonlocal numerical results with molecular dynamics results, while their previous work [31] had clearly shown an effect of chirality on small scale values.

To show the important role of small scale parameter in the mechanical behavior simulation of nanostructures, the variation of the small scale value is a popular procedure that has been employed in many studies. For instance, Yang and Ke [36] and Ke et al. [37] used nonlinear nonlocal Timoshenko beam theory to show the importance of the small scale value to estimate the nonlinear free vibration of single- and double-walled carbon nanotubes with different boundary conditions, respectively. Karaoglu and Aydogdu [38] used nonlocal Euler–Bernoulli beam theory to study the effect of the small scale value on the linear force vibration of single- and double-walled carbon nanotubes. Finally, Sudak [39] showed the dramatic influence of the small scale value on the critical axial strain of double-walled carbon nanotubes.

Hence, all researchers who have used nonlocal continuum theories to simulate the size-dependent mechanical behavior of FG nanobeams have investigated the effects of the small scale parameter on the mechanical behavior of FG nanobeams by changing the value of the small scale parameter [13–15,18,19]. Eltaher et al. [14] changed the value of the square of the small scale parameter ($(e_0a)^2$) from zero to 5×10^{-12} m^2 when they studied the effect of the neutral axis location on the linear natural frequencies of FG nanobeams, while Uymaz [18] and Nazemnezhad and Hosseini-Hashemi [19] used values from 0 to 4×10^{-18} m^2 owing to a lack of information. These researchers implicitly showed that the influence of the small scale parameter on the mechanical behavior of FG nanobeams would be noticeable if the small scale parameter/thickness ratio was equal to or greater than 1 (i.e., $e_0a/h \geq 1$) . Then, in the parametric studies of this work, owing to a lack of information, the small scale (e_0a) is varied from 0 to 2 nm to show the importance of the small scale value on the nonlinear vibration behavior of FG nanobeams.

The selection of a nonlocal continuum mechanics theory, on which are based simulations of the mechanical behavior of nanostructures, is an important factor affecting the accuracy of predictions. Nonlocal Euler–Bernoulli beam theory, the nonlocal parabolic shear deformation beam theory of Reddy, the nonlocal first-order shear deformation beam theory of Timoshenko, and the nonlocal general exponential shear deformation beam theory of Aydogdu are some of the nonlocal beam theories that Aydogdu used to study the static and dynamic responses of homogeneous nanobeams [40]. According to Aydogdu's study [40], one may conclude that the nonlocal Euler–Bernoulli beam theory can predict the mechanical behavior of nanobeams accurately with an increase in the length/thickness ratio (L/h) of nanobeams ($L/h > 20$). Therefore, in the present study, nonlocal nonlinear Euler–Bernoulli beam theory is used to simulate the nonlinear forced vibration of long and narrow ($L/h > 20$) nanobeams.

Another parameter that could significantly affect the accuracy of the predicted mechanical behavior of FG nanobeams is the real position of the neutral axis, which would then be used to derive the governing equations. Eltaher et al. [14] determined the position of the neutral surface of FG micro-/nanobeams based on the concept of neutral surface. In their simulation, the material properties varied continuously through the thickness of the size-dependent beam according to a simple power-law form. Eltaher et al.'s study [14] clearly revealed that with an increase in the difference between the material properties of basic materials of FGMs, such as Young's modulus and mass density, the computational error caused by the elimination of the effect of the exact location of the neutral axis rises. Eltaher et al. [15] also studied the effect of neutral axis position on the dynamic characteristic of thin to moderately thick nanobeams via nonlocal Timoshenko beam modeling. They used a similar concept to obtain the

position of the neutral axis. In the present study, the governing equation is also obtained on the basis of the real position of the neutral axis, which varies with the material composition owing to the importance of the real position of the natural axis in studying the mechanical behavior of FG micro-/nanobeams [14,15].

The study of free and forced vibrations of micro-/nanobeams used in micro- and nanoscale devices that may experience vibration is of great importance. Based on the author's knowledge, there are no notable studies showing the effect of a nonlocal parameter on the mechanical response of FG nanobeams to subharmonic excitation. Thus, the investigation of the effects of the small scale parameter on the steady-state response of FG nanobeams resting on a viscous foundation to subharmonic excitation is the main object of this article. A simple power-law distribution is used to model the variation in the material property graded in the thickness direction. A partial differential equation of motion is derived based on Euler–Bernoulli beam theory, von Karman geometric nonlinearity, and Eringen's nonlocal elasticity theory. To increase the accuracy of the simulation, the real position of the neutral axis, which does not necessarily coincide with the geometric midplane in nonhomogeneous nanobeams, is considered in the derivation of the governing formula as well. The multiple scale method is used to find the governing equations of the steady-state response of FG nanobeams excited by a distributed harmonic force. In the parametric studies of this work, owing to a lack of information, the small scale (e_0a) is varied from 0 to 2 to investigate the effects of the small scale on the steady-state response of excited FG nanobeams.

2 Equation of motion

The dimensionless partial differential equation of motion of a simply supported FG nanobeam resting on a viscous foundation with length L, width b, and thickness h and immovable ends can be derived based on Euler–Bernoulli beam theory, von Karman geometric nonlinearity, and Eringen's nonlocal elasticity theory as follows (see Appendix 1 for details):

$$-\frac{L^4\,(e_0a)^2}{r\,D}\left[-\frac{1}{L^2}\frac{\partial^2 F}{\partial\overline{x}^2}+\frac{\overline{k}r}{L^2}\frac{\partial^2\overline{W}}{\partial\overline{x}^2}+\frac{\overline{c}r}{L^2}\sqrt{\frac{D}{\rho_e L^4}}-\left(\frac{Ar^3}{2L^6}\int_0^1\left(\frac{\partial\overline{W}}{\partial\overline{x}}\right)^2\mathrm{d}\overline{x}\right)\frac{\partial^4\overline{W}}{\partial\overline{x}^4}+\frac{Dr}{L^6}\frac{\partial^4\overline{W}}{\partial\overline{x}^2\partial\overline{t}^2}\right]$$
$$+\frac{\partial^2\overline{W}}{\partial\overline{t}^2}+\frac{\partial^4\overline{W}}{\partial\overline{x}^4}+\frac{\overline{k}L^4}{D}\overline{W}+\frac{\overline{c}L^2}{\sqrt{D\rho_e}}\frac{\partial\overline{W}}{\partial\overline{t}}-\left(\frac{Ar^2}{2D}\int_0^1\left(\frac{\partial\overline{W}}{\partial\overline{x}}\right)^2\mathrm{d}\overline{x}\right)\frac{\partial^2\overline{W}}{\partial\overline{x}^2}=F\frac{L^4}{rD},\tag{1}$$

in which

$$A=\int_{A_0}E\,(z)\,\mathrm{d}A_0,\quad D=\int_{A_0}(z-z_0)^2\,E\,(z)\,\mathrm{d}A_0,\quad \rho_e=\int_{A_0}\rho\,(z)\,\mathrm{d}A_0,\tag{2}$$

$$\overline{x}=\frac{x}{L},\quad \overline{W}=\frac{W}{r},\quad \overline{t}=t\sqrt{D/\rho_e L^4},\tag{3}$$

where $W=W(x,t)$ is the transverse displacement of any point on the geometric midplane of the beam element, $\rho(z)$ and $E(z)$ are the mass density and Young's modulus, respectively, which are functionally graded in the thickness direction, r is the gyration radius of the cross section of the beam, z_0 is the distance of the neutral surface of the FG nanobeam from the geometric midplane of the FG nanobeam, t is time, and A_0 denotes the area of the beam cross section. The stiffness and damping coefficient of the foundation are denoted by $\overline{k}$ and $\overline{c}$, respectively. The transverse loading is given by F.

If the small scale parameter (e_0a) and the power-law index $(\overline{n})$ in Eq. (1) are taken as being equal to zero, then Eq. (1) tends to the well-known local equation of nonlinear lateral vibration of beams obtained and used in some papers [41].

The mode shapes of the linear vibration of nanobeams are used to estimate the transverse displacement of simply supported FG nanobeams:

$$\overline{W} = \sum_{s=1}^{N} \overline{q}_s \left(\overline{t}\right) \sin\left(s\pi\overline{x}\right). \tag{4}$$

Substituting Eq. (4) into Eq. (1) and using Galerkin's method, one can change the partial differential equation into a system of ordinary differential equations:

$$\ddot{\overline{q}}_s + \left(\overline{\omega}_s\right)^2 \overline{q}_s + \overline{C}_s \dot{\overline{q}}_s = -a_s \overline{q}_s \sum_{m=1}^{N} m^2 \left(\overline{q}_m\right)^2 + \left(\overline{F}_s - \left(e_0 a\right)^2 \overline{G}_s\right) \cos\left(\overline{\Omega t}\right), \tag{5}$$

in which

$$\left(\overline{\omega}_s\right)^2 = \frac{\overline{k} L^4}{D} + \frac{\left(s\pi\right)^4}{\frac{\left(e_0 a\right)^2 \left(s\pi\right)^2}{L^2} + 1}, \tag{6a}$$

$$a_s = \frac{Ar^2}{4D} s^2 \pi^4, \tag{6b}$$

$$\overline{C}_s = \frac{\overline{c} L^2}{\sqrt{D\rho_e}}, \tag{6c}$$

$$\overline{F}_s - \left(e_0 a\right)^2 \overline{G}_s = \frac{2L^2}{\left(e_0 a\right)^2 \left(s\pi\right)^2 + L^2} \int_0^1 \left(F\left(\overline{x}\right) \frac{L^4}{rD} - \frac{\left(e_0 a\right)^2 L^2}{rD} \frac{\partial^2 F\left(\overline{x}\right)}{\partial \overline{x}^2} \right) \sin\left(s\pi\overline{x}\right) \mathrm{d}\overline{x}, \tag{6d}$$

and s is the half-wavelength number. $\overline{\omega}_s$ is also the sth dimensionless linear natural frequency of FG nanobeams, which can be obtained by omitting the nonlinear terms and external load from Eq. (1); $\overline{\Omega}$ is the dimensionless working frequency.

3 Solution methodology

The multiple scale method is used to solve the system of ordinary differential equations shown by Eq. (5). Based on the framework of the multiple scale method, $\overline{q}_s$ is defined as

$$\overline{q}_s = \varepsilon \overline{q}_{s1}\left(T_0, T_2\right) + \varepsilon^3 \overline{q}_{s3}\left(T_0, T_2\right), \tag{7}$$

where ε is a small dimensionless parameter, $T_0 = \overline{t}$, and $T_2 = \varepsilon^2 \overline{t}$. As is seen, both the slow scale $T_1 = \varepsilon \overline{t}$ and the term $\varepsilon^2 \overline{q}_{s2}$ are eliminated from Eq. (7) because the nonlinear terms in Eq. (5) are cubic [42]. It is necessary to show the damping terms and the nonlinear terms in the same perturbation equations to study the sub- or superharmonic response of vibrating FG nanobeams, while the excitation terms must be shown in equations resulting from equating the coefficient of ε^1. Hence, the damping coefficients ($\overline{C}_s$) must be set to $2\varepsilon^2 \hat{C}_s$, and the excitation is not changed. The following equations are obtained by inserting Eq. (7) into Eq. (5) and equating the coefficients of ε^1 and ε^3 on both sides:

$$D_0^2 \overline{q}_{s1} + \left(\overline{\omega}_s\right)^2 \overline{q}_{s1} = \left(\hat{F}_s - \left(e_0 a\right)^2 \hat{G}_s\right) \cos\left(\overline{\Omega t}\right), \tag{8}$$

$$D_0^2 \overline{q}_{s3} + 2 D_0 D_2 \overline{q}_{s1} + \left(\overline{\omega}_s\right)^2 \overline{q}_{s3} + 2\hat{C}_s D_0 \overline{q}_{s1} = -a_s \overline{q}_{s1} \sum_{m=1}^{N} m^2 \overline{q}_{m1}^2, \tag{9}$$

where $D_n = \frac{\partial}{\partial T_n}$. Substituting the solution of Eq. (8), which can be expressed as $\overline{q}_{s1} = A_s\left(T_2\right) \exp\left(i\overline{\omega}_s T_0\right) + \Lambda_s \exp\left(i\overline{\Omega} T_0\right) + CC$, into Eq. (9) yields

$$D_0^2 \overline{q}_{s3} + \left(\overline{\omega}_s\right)^2 \overline{q}_{s3} = -\left(i\overline{\omega}_s 2\hat{C}_s A_s \exp\left(i\overline{\omega}_s T_0\right) + i\hat{C}_s \overline{\Omega} \Lambda_s \exp\left(i\overline{\Omega} T_0\right) \right)$$

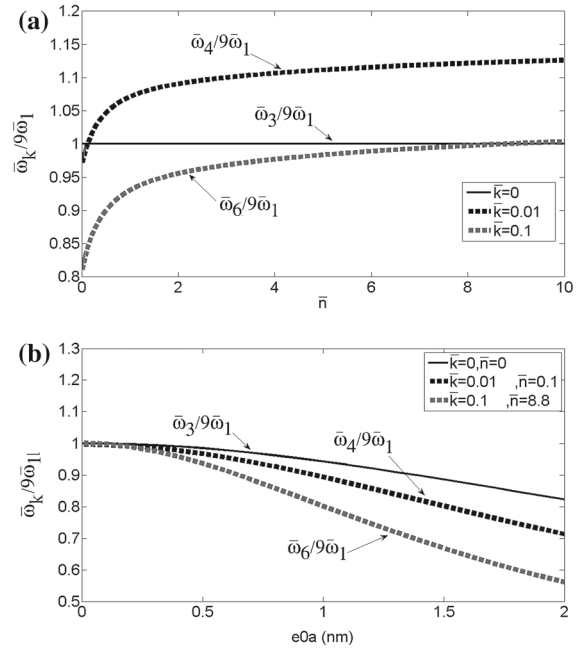

Fig. 1 Effect of **a** power-law index ($e_0a = 0$); **b** small scale parameter on possibility of occurrence of sub- and superharmonic responses simultaneously

$$-\left(i2\overline{\omega}_s \frac{\mathrm{d}A_s}{\mathrm{d}T_2}\exp\left(i\overline{\omega}_s T_0\right)\right) - a_s \sum_{m=1}^{N} m^2 \left(\overline{q}_{s1}\overline{q}_{m1}^2\right) + CC, \tag{10}$$

where

$$\begin{aligned}
\overline{q}_{s1}\overline{q}_{m1}^2 = {} & 2A_sA_m\Lambda_m \exp\left(iT_0\left(\overline{\omega}_m+\overline{\omega}_s+\overline{\Omega}\right)\right) + A_m^2A_s\exp\left(iT_0\left(2\overline{\omega}_m+\overline{\omega}_s\right)\right) + 2A_m\overline{A}_mA_s\exp\left(i\overline{\omega}_sT_0\right) \\
& + A_s\Lambda_m^2\exp\left(iT_0\left(\overline{\omega}_s+2\overline{\Omega}\right)\right) + 2A_s\Lambda_m^2\exp\left(iT_0\overline{\omega}_s\right) + A_m^2\overline{A}_s\exp\left(iT_0\left(2\overline{\omega}_m-\overline{\omega}_s\right)\right) \\
& + 2A_sA_m\Lambda_m\exp\left(iT_0\left(\overline{\omega}_m+\overline{\omega}_s-\overline{\Omega}\right)\right) + A_s\Lambda_m^2\exp\left(iT_0\left(\overline{\omega}_s-2\overline{\Omega}\right)\right) + 2A_s\overline{A}_m\Lambda_m\exp\left(iT_0\left(\overline{\omega}_s-\overline{\omega}_m-\overline{\Omega}\right)\right) \\
& + 2A_s\overline{A}_m\Lambda_m\exp\left(iT_0\left(-\overline{\omega}_m+\overline{\omega}_s+\overline{\Omega}\right)\right) + A_m^2\Lambda_s\exp\left(iT_0\left(2\overline{\omega}_s+\overline{\Omega}\right)\right) + \Lambda_s\Lambda_m^2\exp\left(iT_0\left(3\overline{\Omega}\right)\right) \\
& + 2A_m\Lambda_m\Lambda_s\exp\left(iT_0\left(2\overline{\Omega}+\overline{\omega}_m\right)\right) + 3\Lambda_m^2\Lambda_s\exp\left(iT_0\left(\overline{\Omega}\right)\right) + 4A_m\Lambda_m\Lambda_s\exp\left(iT_0\left(\overline{\omega}_m\right)\right) \\
& + 2A_m\overline{A}_m\Lambda_s\exp\left(iT_0\left(\overline{\Omega}\right)\right) + \overline{A}_m^2\Lambda_s\exp\left(iT_0\left(-2\overline{\omega}_m+\overline{\Omega}\right)\right) + 2\overline{A}_m\Lambda_s\Lambda_m\exp\left(iT_0\left(2\overline{\Omega}-\overline{\omega}_m\right)\right) + CC,
\end{aligned} \tag{11}$$

in which CC stands for the complex conjugate of the preceding terms and

$$\Lambda_s = \frac{\left(\hat{F}_s - (e_0a)^2\,\hat{G}_s\right)}{2\left(\overline{\omega}_s^2 - \overline{\Omega}^2\right)}.$$

As seen, if $\overline{\Omega} \approx 3\overline{\omega}_n$ when $\overline{\omega}_k \approx 9\overline{\omega}_n$, a combination of subharmonic and superharmonic responses may occur simultaneously. The possibility of the occurrence of combination resonances ($\overline{\omega}_p + \overline{\omega}_q \approx 2\overline{\Omega}$) must be considered as well.

A case study on the natural frequencies of FG nanobeams made of silicon nitride (Si_3N_4) and stainless-steel grade 304 (SUS304) showed that the stiffness of the foundation, material composition, and small scale value affect the response of an excited FG nanobeam. In this study, it is assumed that the working frequency is almost three times as great as the first natural frequency (i.e., $\overline{\Omega} \approx 3\overline{\omega}_1$). It is also assumed that the nanobeam is constructed of pure metal when the power-law index ($\overline{n}$) is zero. On the basis of Fig. 1a, as reported by Nayfeh and Mook [42], if the stiffness of the foundation approaches zero, the third natural frequency ($\overline{\omega}_3$) will be close to nine times as much as the first frequency ($\overline{\omega}_1$) (i.e., $\overline{\omega}_3 \approx 9\overline{\omega}_1$). This means that sub- and superharmonic responses occur

Table 1 Effects of small scale parameter on possibility of closeness of $\overline{\omega}_k$ to $9\overline{\omega}_1$ and occurrence of combination resonances

$\overline{k}$ (nN/nm^2)	$\overline{n}$ (case study)	e_0a (nm)	$\overline{\omega}_k$	$\overline{\omega}p + \overline{\omega}_q \approx 6\overline{\omega}_1$
0.01	0.1	0–0.4	$\overline{\omega}_4 \approx 9\overline{\omega}_1$	No
0.01	0.1	1.7–2	$\overline{\omega}_5 \approx 9\overline{\omega}_1$	$\overline{\omega}_2 + \overline{\omega}_3 \approx 6\overline{\omega}_1$
0.03	0.1	0–0.3	$\overline{\omega}_5 \approx 9\overline{\omega}_1$	No
0.03	0.1	1.4	$\overline{\omega}_6 \approx 9\overline{\omega}_1$	No
0.03	0.1	1.9–2	$\overline{\omega}_7 \approx 9\overline{\omega}_1$	$\overline{\omega}_2 + \overline{\omega}_4 \approx 6\overline{\omega}_1$

Table 2 Effects of stiffness of foundation and material composition on possibility of simultaneous occurrence of sub- and superharmonic responses with combination resonances. ($e_0a = 0$)

$\overline{k}$ (nN/nm^2)	$\overline{n}$ (case study)	The possibility of occurrence of a combination of sub- and superharmonic resonances	Possibility of occurrence of combination resonances
0.01	0–0.2	Yes $\overline{\omega}_4 \approx 9\overline{\omega}_1$	No
0.01	10	No	No
0.03	0–0.1	Yes $\overline{\omega}_5 \approx 9\overline{\omega}_1$	No
0.03	9.7–10	No	Yes $\overline{\omega}_2 + \overline{\omega}_3 \approx 6\overline{\omega}_1$
0.05	9–10	Yes $\overline{\omega}_5 \approx 9\overline{\omega}_1$	No
0.05	0–0.2	No	Yes$\overline{\omega}_2 + \overline{\omega}_4 \approx 6\overline{\omega}_1$
0.1	8.8–10	Yes $\overline{\omega}_6 \approx 9\overline{\omega}_1$	No
0.1	0–1	No	Yes$\overline{\omega}_3 + \overline{\omega}_4 \approx 6\overline{\omega}_1$
0.2	10	Yes $\overline{\omega}_7 \approx 9\overline{\omega}_1$	No

simultaneously. Examination of FG nanobeams reveals that the material composition makes no difference in this ratio (Fig. 1a). In this case, combination resonances may not occur. Figure 1b clearly reveals that at a fixed value of the power-law index, an increase in the small scale parameter increases the difference between $\overline{\omega}_k$, which is close to $9\overline{\omega}_1$ at $e_0a = 0$ and $9\overline{\omega}_1$, while it decreases the difference between $\overline{\omega}_k$, which is far from $9\overline{\omega}_1$ at $e_0\, a = 0$, and $9\overline{\omega}_1$ (Table 1). On the other hand, the simultaneous occurrence of sub- and superharmonic responses with combination resonances depends on the material compositions and the stiffness of the foundation (Table 2).

It is worth mentioning that other linear combinations of frequencies appearing in Eq. (11) may make secular terms of particular solutions to Eq. (10) depending on the stiffness of the foundation and the material compositions. For example, a FG nanobeam ($\overline{n} = 0.1$) resting on a foundation whose stiffness coefficient is 0.03nN/nm^2 is considered. In that case, not only $\overline{\omega}_5 \approx 9\overline{\omega}_1$ but also $\overline{\omega}_3 + \overline{\omega}_5 - \overline{\Omega} \approx \overline{\omega}_5$; while $\overline{\omega}_2 + \overline{\omega}_3 \approx 2\overline{\Omega}$ as well as $\overline{\omega}_4 \approx 9\overline{\omega}_1$ can only be seen if the stiffness of the foundation decreases to 0.01 nN/nm^2.

4 Combination of subharmonic and superharmonic responses

It is assumed that $\overline{\Omega} \approx 3\overline{\omega}_1$ and $\overline{\omega}_k$, which is close to $9\overline{\omega}_1$, occurs. The detuning parameters σ and σ_1 are introduced to define $\overline{\Omega} = 3\overline{\omega}_1 + \varepsilon^2\sigma$ and $3\overline{\Omega} = \overline{\omega}_k + \varepsilon^2\sigma_1$, respectively. It is also assumed that linear combinations of frequencies that appear in Eq. (11) are far from $\overline{\omega}_1$ and $\overline{\omega}_k$.

The steady-state motion can be expressed as follows (for details and definitions of parameters, see Appendix 2):

$$\left(\frac{3}{4}a_1\Lambda_1\alpha_1^2\right)^2 = \left(-\frac{1}{3}\sigma\alpha_1\overline{\omega}_1 + a_1\alpha_1\sum_{m=2}^{N} m^2\Lambda_m^2 + \frac{k^2}{4}\alpha_1 a_1\alpha_k^2 + 3a_1\Lambda_1^2\alpha_1 + \frac{3}{8}a_1\alpha_1^3\right)^2 + \left(\hat{C}_1\alpha_1\overline{\omega}_1\right)^2, \qquad (12)$$

$$\left(a_k\Lambda_k\sum_{m=1}^{N}m^2\Lambda_m^2\right)^2=\left(-\alpha_k\sigma_1\overline{\omega}_k+\frac{3}{8}a_kk^2\alpha_k^3+\frac{1}{4}a_k\alpha_k\alpha_1^2+a_k\alpha_k\sum_{m=1}^{N}m^2\Lambda_m^2+2k^2a_k\Lambda_k^2\alpha_k\right)^2+\left(\hat{C}_k\alpha_k\overline{\omega}_k\right)^2. \tag{13}$$

According to Eqs. (12) and (13), these two solutions are possible: either $\alpha_1 = 0$, and $\alpha_k \neq 0$, or $\alpha_1 \neq 0$, and $\alpha_k \neq 0$.

The following equation expresses the time-dependent lateral deflection of a vibrating FG nanobeam:

$$\begin{aligned}\overline{W}\left(\overline{x},\overline{t}\right) &= \varepsilon\alpha_1\cos\left(\frac{1}{3}\overline{\Omega t}-\frac{1}{3}\gamma_1\right)\sin\left(\pi\overline{x}\right)+\varepsilon\alpha_k\cos\left(3\overline{\Omega t}-\gamma_2\right)\sin\left(k\pi\overline{x}\right)\\ &\quad+2\varepsilon\sum_{n=1}^{N}\Lambda_n\cos\left(\overline{\Omega t}\right)\sin\left(n\pi\overline{x}\right)+O\left(\varepsilon^3\right).\end{aligned} \tag{14}$$

5 Combination resonances

It is also assumed that there are two frequencies that satisfy $\overline{\omega}_p+\overline{\omega}_q\approx 2\overline{\Omega}$ as well as $\overline{\Omega}\approx 3\overline{\omega}_1$, and $\overline{\omega}_k$, which is close to $9\overline{\omega}_1$, occurs. It is also supposed that linear combinations of frequencies that appear in Eq. (11) are far from $\overline{\omega}_1$, $\overline{\omega}_k$, $\overline{\omega}_p$ and $\overline{\omega}_q$. The detuning parameters σ, σ_1 and σ_2 are introduced to define $\overline{\Omega}=3\overline{\omega}_1+\varepsilon^2\sigma$, $3\overline{\Omega}=\overline{\omega}_k+\varepsilon^2\sigma_1$ and $2\overline{\Omega}=\overline{\omega}_p+\overline{\omega}_q+\varepsilon^2\sigma_2$, respectively.

In this case, the possible solutions are as follows (for details and definitions of parameters, see Appendix 3):

(a) $\alpha_1=\alpha_p=\alpha_q=0$, and $\alpha_k\neq 0$;
(b) $\alpha_1\neq 0$,and$\alpha_k\neq 0$, but $\alpha_p=\alpha_q=0$;
(c) $\alpha_1=0$, and $\alpha_k\neq 0$, $\alpha_p\neq 0$, and $\alpha_q\neq 0$;
(d) $\alpha_1\neq 0$, $\alpha_k\neq 0$, $\alpha_p\neq 0$, and $\alpha_q\neq 0$.

The lateral deflection of a vibrating FG nanobeam can be represented by the following equation:

$$\begin{aligned}\overline{W}\left(\overline{x},\overline{t}\right) &= \varepsilon\alpha_1\cos\left(\frac{1}{3}\overline{\Omega t}-\frac{1}{3}\gamma_1\right)\sin\left(\pi\overline{x}\right)+\varepsilon\alpha_k\cos\left(3\overline{\Omega t}-\gamma_2\right)\sin\left(k\pi\overline{x}\right)+\varepsilon\alpha_p\cos\left(\overline{\omega}_p\overline{t}+\beta_P\right)\sin\left(p\pi\overline{x}\right)\\ &\quad+\varepsilon\alpha_q\cos\left(\overline{\omega}_q\overline{t}+\beta_q\right)\sin\left(q\pi\overline{x}\right)+2\varepsilon\sum_{n=1}^{N}\Lambda_n\cos\left(\overline{\Omega t}\right)\sin\left(n\pi\overline{x}\right)+O\left(\varepsilon^3\right).\end{aligned} \tag{15}$$

It can be concluded that the formulas governing cases (a) and (b) are in accordance with those governing the possible solutions mentioned in Sect. 4.

6 Validation

Nayfeh and Mook [42] used the multiple scale method to study the steady-state motion of a simply supported beam with subharmonic excitation. They used linear mode shapes of simply supported beams expressed as $\sqrt{2}\sin\left(s\pi\overline{x}\right)$. The solutions proposed by Nayfeh and Mook [42] were used to verify the presented equations. For this purpose, the value of the small scale parameter (e_0a), the power-law index ($\overline{n}$), and the coefficient of the stiffness of the foundation ($\overline{k}$) in all equations were set to zero. It was also assumed that $\overline{\Omega}=3\overline{\omega}_1+\varepsilon^2\sigma$. According to the aforementioned assumptions, three times the working frequency is close to the third natural frequency (i.e., $3\overline{\Omega}\approx\overline{\omega}_3$). Thus, Eqs. (6a) and (6b) change to $(\overline{\omega}_s)^2=(s\pi)^4$ and $a_s=\frac{1}{4}s^2\pi^4$, respectively. It must be mentioned that the coefficient of a_s is half that used by Nayfeh and Mook [42] because of the difference between the coefficients of the linear mode shapes that were used.

The following equations, which are in agreement with those proposed by Nayfeh and Mook [42], are obtained by substituting the new expression of $\overline{\omega}_s$ and a_s into Eqs. (65)–(68).

$$\hat{C}_1\alpha_1\overline{\omega}_1 + \frac{3}{16}\pi^2\Lambda_1\alpha_1^2\sin\gamma_1 = 0, \tag{16}$$

$$-\sigma\alpha_1 + \frac{3}{4}\pi^2\alpha_1\sum_{m=2}^{N} m^2\Lambda_m^2 + \frac{9}{16}\pi^2\alpha_1^2\Lambda_1\cos(\gamma_1) + \frac{27}{16}\pi^2\alpha_1\alpha_3^2 + \frac{9}{4}\pi^2\Lambda_1^2\alpha_1 + \frac{9}{32}\pi^2\alpha_1^3 = 0, \tag{17}$$

$$\hat{C}_3\alpha_3 + \frac{\pi^2}{4}\Lambda_k\sum_{m=1}^{N} m^2\Lambda_m^2\sin\gamma_2 = 0, \tag{18}$$

$$-3\alpha_3\sigma + \frac{\pi^2}{4}\Lambda_k\sum_{m=1}^{N} m^2\Lambda_m^2\cos\gamma_2 + \frac{27}{32}\pi^2\alpha_k^3 + \frac{\pi^2}{16}\alpha_k\alpha_1^2 + \frac{\pi^2}{4}\alpha_k\sum_{m=1}^{N} m^2\Lambda_m^2 + \frac{9\pi^2}{2}\Lambda_k^2\alpha_k = 0. \tag{19}$$

7 Results

In this section, four possible solutions, mentioned in Sect. 5, are discussed analytically and numerically because they include the possible solutions indicated in Sect. 4. In this section, the stiffness of the foundation is set to 0.01 nN/nm^2, and it is assumed that the damping coefficient of the foundation is small. All the numerical data are obtained based on a continuous harmonic lateral force with constant intensity as well.

7.1 Possible solution (a)

In this case, the following equations, which represent the superharmonic response of a vibrating FG nanobeam, govern the peak response and corresponding detuning:

$$\alpha_k = \frac{a_k\Lambda_k\sum_{m=1}^{N} m^2\Lambda_m^2}{\overline{\omega}_k\widehat{C}_k}, \tag{20}$$

$$\overline{\omega}_k\sigma_1 = \frac{3}{8}k^2\frac{a_k^3\Lambda_k^2\left(\sum_{m=1}^{N} m^2\Lambda_m^2\right)^2}{\overline{\omega}_k^2\widehat{C}_k^2} + 2a_kk^2\Lambda_k^2 + a_k\sum_{m=1}^{N} m^2\Lambda_m^2. \tag{21}$$

Based on Table 1, the small scale affects the order of the frequency involved in the steady-state response of the FG nanobeam. The fourth frequency ($\overline{\omega}_4$) will be expected to be seen in the steady-state response of the FG nanobeam if the small scale parameter is close to zero. According to Eq. (6d) and the assumptions mentioned earlier, Λ_4 is zero. Hence, α_4 will be zero. Then, the lateral deflection of the FG nanobeam is

$$\overline{W}(\overline{x},\overline{t}) = 2\varepsilon\sum_{n=1}^{N}\Lambda_n\cos(\overline{\Omega t})\sin(n\pi\overline{x}) + O(\varepsilon^3). \tag{22}$$

Figure 2 clearly demonstrates that in this situation, the lateral deflection of the FG nanobeam is similar to the first mode shape of its linear free vibration. It is also seen that with an increase in the small scale value and power-law index, the deflection of the nanobeam decreases.

On the other hand, the fifth frequency ($\overline{\omega}_5$) of the FG nanobeam can be seen in the steady-state response if the small scale parameter approaches 2 nm. Figure 3 clearly shows that with a rise in the small scale value or a decrease in the power-law index, the peak response increases. In this situation, the time-dependent lateral deflection of the FG nanobeam can be represented by

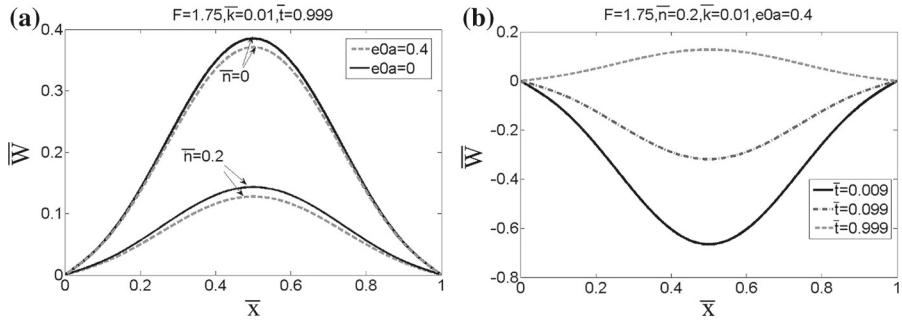

Fig. 2 **a** Effect of small scale and power-law index on lateral deflection of vibrating FG nanobeam. **b** Variation of lateral deflection of FG nanobeam with time (based on Eq. 22)

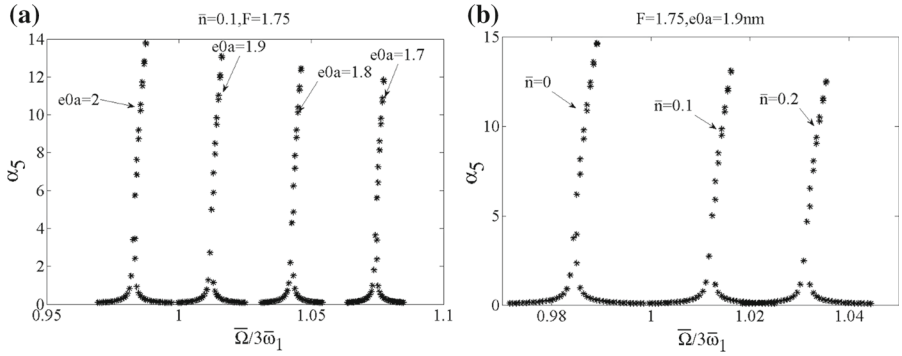

Fig. 3 Effect of **a** small scale parameter and **b** power-law indexon frequency-response curves

$$\overline{W}\left(\overline{x},\overline{t}\right)=\varepsilon\alpha_5\cos\left(3\overline{\Omega t}-\gamma_2\right)\sin\left(5\pi\overline{x}\right)+2\varepsilon\sum_{n=1}^{N}\Lambda_n\cos\left(\overline{\Omega t}\right)\sin\left(n\pi\overline{x}\right)+O\left(\varepsilon^3\right),\tag{23}$$

where $\sin\gamma_2=-\hat{C}_5\alpha_5\overline{\omega}_5/a_5\Lambda_5\sum_{m=1}^{N}m^2\Lambda_m^2$.

Figure 4, which shows the lateral deflection of FG nanobeams at its peak response, reveals that in this case the effect of the small scale value on the frequency of response is more than that of the power-law index (compare Fig. 4a with Fig. 4b). The presence of the fifth mode shape in the configuration of the time-dependent lateral deflection of the nanobeam is observed (Fig. 4c, d). A comparison of Fig. 4c, d with Fig. 2a, b shows how the value of the small scale can significantly change the response of the FG nanobeam.

7.2 Possible solution (b)

Based on the given values of σ_1 and σ, one can use the following nonlinear equations to find the amplitude of the mode shapes involved in the response of the FG nanobeam:

$$\begin{aligned}&\left(\hat{C}_1\overline{\omega}_1\right)^2+\left(-\frac{1}{3}\sigma\overline{\omega}_1+a_1\sum_{m=1}^{N}m^2\Lambda_m^2+3a_1\Lambda_1^2\right)^2+\left(\frac{3}{8}a_1\right)^2\alpha_1^4+\left(\frac{1}{4}a_1k^2\right)^2\alpha_k^4+\left(\frac{3}{16}a_1^2k^2\right)^2\alpha_1^2\alpha_k^2\\&+\left[\left(\frac{3}{4}a_1\right)\left(-\frac{1}{3}\sigma\overline{\omega}_1+a_1\sum_{m=1}^{N}m^2\Lambda_m^2+3a_1\Lambda_1^2\right)-\left(\frac{3}{4}a_1\Lambda_1\right)^2\right]\alpha_1^2\\&+\left(\frac{a_1k^2}{2}\right)\left(-\frac{1}{3}\sigma\overline{\omega}_1+a_1\sum_{m=1}^{N}m^2\Lambda_m^2+3a_1\Lambda_1^2\right)\alpha_k^2+\left(\frac{a_1k^2}{4}\right)^2\alpha_k^4=0,\end{aligned}\tag{24}$$

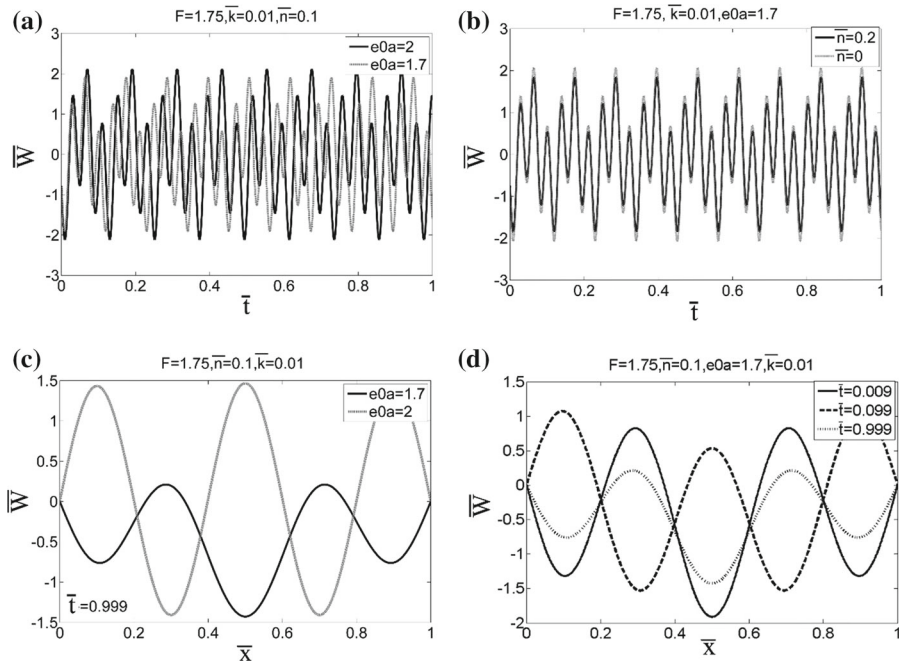

Fig. 4 Time-dependent variations of lateral deflection of middle point of FG nanobeam **a** with different small scale value, **b** with different power-law index; **c** effect of small scale value on lateral deflection of FG nanobeam, **d** variation of lateral deflection of FG nanobeam with time (based on Eq. 23)

$$\left[\left(-\overline{\omega}_k\sigma_1 + a_k\sum_{m=1}^{N} m^2\Lambda_m^2 + 2a_k k^2\Lambda_k^2\right)\alpha_k + \left(\frac{3k^2a_k}{8}\right)\alpha_k^3 + \frac{a_k}{4}\alpha_k\alpha_1^2\right]^2 - \left(a_k\Lambda_k\sum_{m=1}^{N} m^2\Lambda_m^2\right)^2 + \left(\overline{\omega}_k\hat{C}_k\right)^2\alpha_k^2 = 0. \tag{25}$$

Based on the assumptions used in this section, if the small scale value is near zero, the only possible solution of α_4 is zero because of the disappearance of Λ_4 from Eq. (25). In this situation, a subharmonic response may be seen. If there is a subharmonic response, the minimum value of α_1 and the corresponding detuning can be found via the following equations:

$$\alpha_1^2 = 16\left(\hat{C}_1\overline{\omega}_1\right)^2 \Big/ (3a_1\Lambda_1)^2, \tag{26}$$

$$\sigma = \frac{3}{\overline{\omega}_1}\left(\frac{8\left(\hat{C}_1\overline{\omega}_1\right)^2}{3a_1\Lambda_1^2} + a_1\sum_{m=2}^{N} m^2\Lambda_m^2 + 3a_1\Lambda_1^2\right). \tag{27}$$

Figure 5 demonstrates the effect of the power-law index on the frequency response of FG nanobeams in these conditions. The small scale value does not significantly affect the frequency response owing to the small value of the small scale parameter. The minimum value of α_1 is 62.88 when the small scale is zero and decreases by 0.1 % if the small scale increases to 0.4 nm.

According to Table 1, if the small scale value is near 2 nm, it will be expected that the first ($\overline{\omega}_1$) and the fifth ($\overline{\omega}_5$) frequencies of FG nanobeam will be seen in the time-dependent lateral deflection of the FG nanobeam. Figure 6 demonstrates the effects of the small scale parameter on the frequency response of FG nanobeams. It can be concluded that the smallest difference between the working frequency ($\overline{\Omega}$) and the first natural frequency ($\overline{\omega}_1$) in which the steady-state response involves the first and fifth frequencies of the FG nanobeam is dependent on the

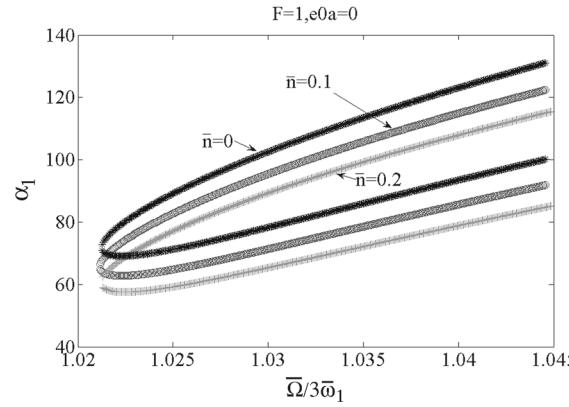

Fig. 5 Effect of power-law index on frequency response of FG nanobeams in subharmonic response

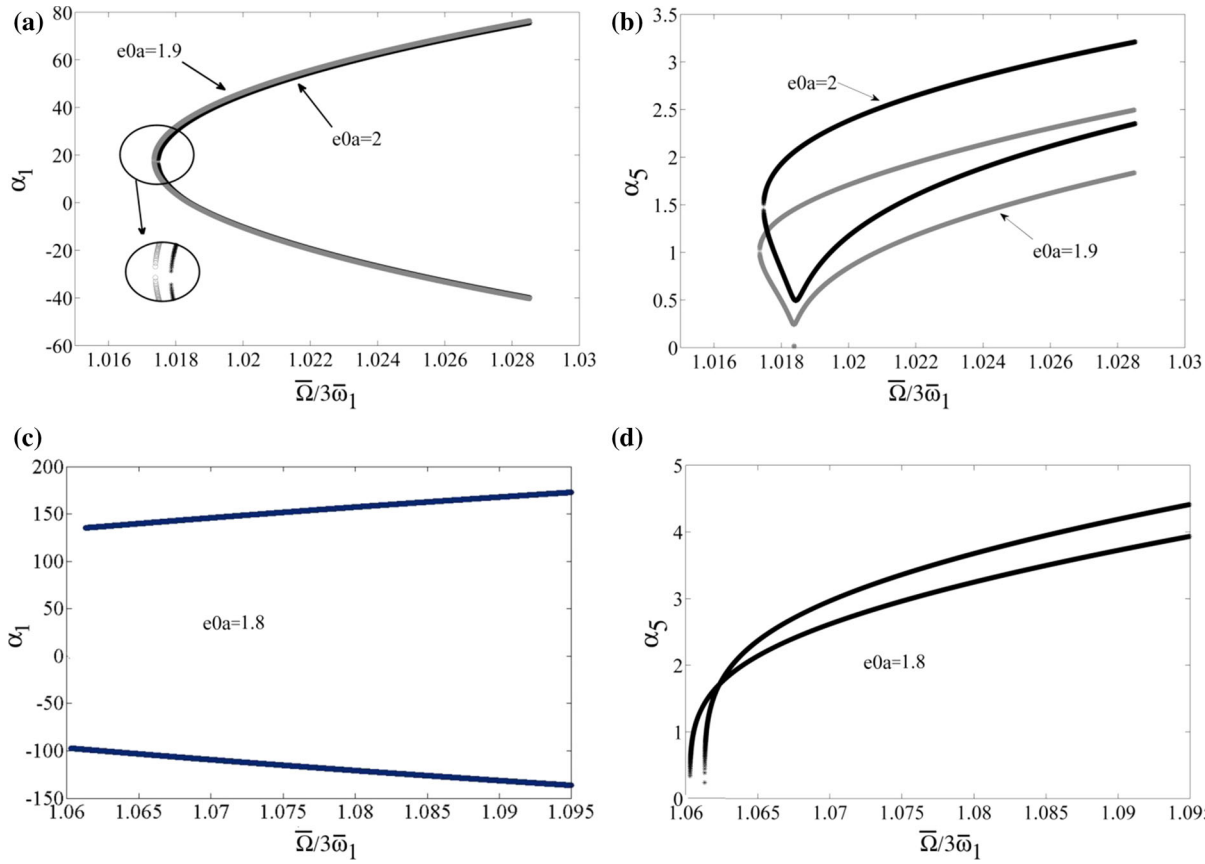

Fig. 6 Effects of small scale parameter on frequency response of FG nanobeams (F = 1, $\overline{n} = 0.1$)

small scale value. The only possible response will be superharmonic (Fig. 3) if the $\overline{\Omega}/3\overline{\omega}_1$ ratio is smaller than the minimum value shown in Fig. 6.

Figure 7 clearly reveals that a rise in the power-law index decreases the amplitude of the involved frequencies. According to Figs. 6 and 7, the amplitude of the first frequency is dominant.

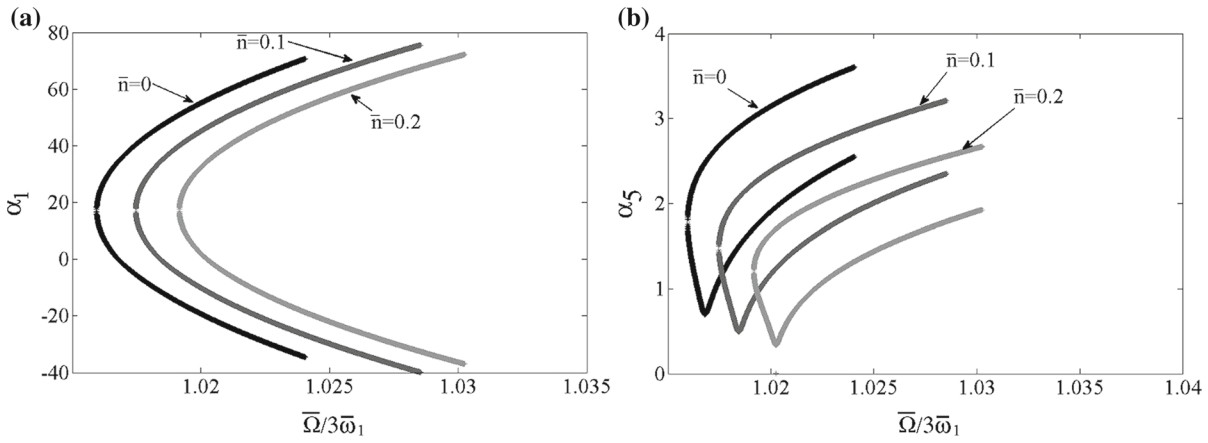

Fig. 7 Effects of power-law index on frequency response of FG nanobeams ($F = 1$, $e_0a = 2$)

7.3 Possible solutions (c) and (d)

By omitting trigonometric functions from Eqs. (78)–(86) and setting the value of α_1 to zero, one can obtain the following compact equations, which are useful for finding the amplitude of the mode shapes involved in the response of FG nanobeams when $\alpha_1 = 0$, $\alpha_k \neq 0$, $\alpha_p \neq 0$, and $\alpha_q \neq 0$:

$$\alpha_p^2 = Q\alpha_q^2, \tag{28}$$

$$\left\{\left[\left(\frac{a_p q^2}{4\overline{\omega}_p} + \frac{3q^2 a_q}{8\overline{\omega}_q}\right) + Q\left(\frac{a_q p^2}{4\overline{\omega}_q} + \frac{3p^2 a_p}{8\overline{\omega}_p}\right)\right]\alpha_q^2 + \left(\frac{k^2 a_p}{4\overline{\omega}_p} + \frac{k^2 a_q}{4\overline{\omega}_q}\right)\alpha_k^2 + \left[\left(\frac{a_p}{\overline{\omega}_p} + \frac{a_q}{\overline{\omega}_q}\right)\sum_{m=1}^{N} m^2\Lambda_m^2 - \sigma_2 + 2\left(p^2 a_p \Lambda_p^2 + q^2 a_q \Lambda_q^2\right)\right]\right\}^2 + \left(\hat{C}_p + \hat{C}_q\right)^2 - f = 0, \tag{29}$$

$$\left[\left(-\overline{\omega}_k\sigma_1 + a_k\sum_{m=1}^{N} m^2\Lambda_m^2 + 2a_k k^2\Lambda_k^2\right)\alpha_k + \left(\frac{3k^2 a_k}{8}\right)\alpha_k^3 + \frac{a_k}{4}\left(Qp^2 + q^2\right)\alpha_k\alpha_q^2\right]^2 - \left(a_k\Lambda_k\sum_{m=1}^{N} m^2\Lambda_m^2\right)^2 + \left(\overline{\omega}_k\hat{C}_k\right)^2\alpha_k^2 = 0, \tag{30}$$

in which

$$Q = \frac{\overline{\omega}_q\hat{C}_q a_p}{\overline{\omega}_p\hat{C}_p a_q}, \tag{31}$$

$$f = \left(\frac{a_p\Lambda_p\Lambda_q}{\overline{\omega}_p}\right)^2 Q^{-1} + \left(\frac{a_q\Lambda_p\Lambda_q}{\overline{\omega}_q}\right)^2 Q + 2\frac{a_p a_q\Lambda_p^2\Lambda_q^2}{\overline{\omega}_p\overline{\omega}_q}. \tag{32}$$

The second ($\overline{\omega}_2$) and third ($\overline{\omega}_3$) frequencies are involved in the combined response when the small scale is close to 2 nm on the basis of the assumptions mentioned earlier and Table 1. According to Eq. (6d), Λ_2 is zero because it is assumed that the density of the distributed lateral load is constant. Then one can conclude that α_2 and α_3 must be zero because of the disappearance of $'f'$ from Eq. (29). Hence, this case does not occur in FG nanobeams whose power-law index is 0.1 and that rest on a foundation whose stiffness coefficient is 0.01 nN/nm^2. A similar conclusion can be drawn when it is expected that $\alpha_1 \neq 0$.

8 Conclusions

This article examined the effects of a small scale parameter on the steady-state response of FG nanobeams resting on a viscous foundation to subharmonic excitation. Euler–Bernoulli beam theory, von Karman geometric nonlinearity, and Eringen's nonlocal elasticity theory were used to derive the partial differential equation of motion of FG nanobeams whose material property was graded in the thickness direction. It was assumed that the working frequency was almost three times as great as the first natural frequency of a FG nanobeam (i.e., $\overline{\Omega} \approx 3\overline{\omega}_1$). The study was conducted in two stages. First, the relationship among natural frequencies was examined, and then the equation governing the general response of excited FG nanobeams was derived via the multiple scale method. The results clearly revealed that the relationship among the natural frequencies was completely dependent on the small scale parameter, material composition, and foundation stiffness. Although the simplest response of a FG nanobeam is only a subharmonic response or superharmonic response, there is the possibility of occurrence of a superharmonic or combination resonances as well as a subharmonic response in some combinations of small scale values, power-law index, and foundation stiffness. It is also worth mentioning that with fixed values of the power-law index and foundation stiffness, the number of frequencies involved in a superharmonic response and combination resonances may vary with the small scale value. According to the results, in a superharmonic response, the peak response increases as the small scale value increases or the power-law index decreases, while in a subharmonic response, the effect of the small scale parameter on the frequency response is negligible. It was also seen that in cases where subharmonic and superharmonic responses are combined, the amplitude of the subharmonic response is dominant.

Acknowledgements The author gratefully acknowledges the support of Yasouj University under grant Gryu-89111109.

Appendix 1

The equations of motion of a simply supported FG nanobeam with length L, width b, and thickness h and immovable ends can be derived using Hamilton's principle. In this study, based on previous research [19,21], it is assumed that the in-plane inertia and rotary inertia are negligible:

$$\frac{\partial \hat{N}}{\partial x} = 0, \tag{33}$$

$$F - \overline{k}W - \overline{c}\frac{\partial W}{\partial t} - \frac{\partial^2 \hat{M}}{\partial x^2} + \hat{N}\frac{\partial^2 W}{\partial x^2} = \left(\int_{A_0} \rho\,(z)\,\mathrm{d}A_0\right)\frac{\partial^2 W}{\partial t^2}, \tag{34}$$

where $W = W(x,t)$ is the transverse displacement of any point on the geometric midplane of the FG nanobeam element, $\rho(z)$ is the mass density, which is functionally graded in the thickness direction, $\hat{N}$ is the axial normal force, $\hat{M}$ is the bending moment, $\overline{k}$ is the stiffness of the foundation, $\overline{c}$ is the damping coefficient of the foundation, and $F = F\,(x)\cos\,(\Omega t)$ is the transverse loading. A_0 denotes the area of the FG nanobeam cross section.

According to the Euler–Bernoulli hypothesis and von Karman type geometrical nonlinearity, the strain displacement relationship is as follows [19,21]:

$$\varepsilon_x = \frac{\partial u_1}{\partial x} + \frac{1}{2}\left(\frac{\partial W}{\partial x}\right)^2, \tag{35}$$

where u_1 is the total displacement along the x-direction given by Eq. (36):

$$u_1\,(x,z,t) = u_0\,(x,t) - (z - z_0)\,\frac{\partial W}{\partial x}, \tag{36}$$

where $u_0\,(x,t)$ is an axial displacement of any point on the geometric midplane of the FG nanobeam element, and z_0 is the distance between the neutral surface and the geometric midplane of the FG nanobeam (Fig. 8) [14].

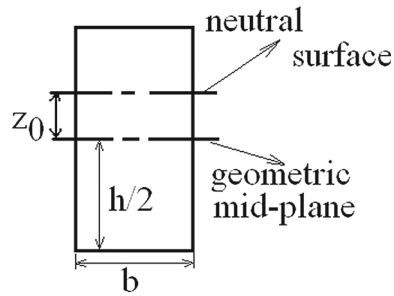

Fig. 8 Cross section of functionally graded beam showing distance of neutral surface from geometric midplane

According to the physical concept of a neutral surface, z_0 can be written as follows [14] (details can be found in Ref. [14]):

$$z_0 = \int_{A_0} zE\,(z)\,\mathrm{d}A_0 \Big/ \int_{A_0} E\,(z)\,\mathrm{d}A_0. \tag{37}$$

Based on Eringen's nonlocal elasticity, the stress–strain relationship is

$$\sigma_x - (e_0 a)^2\,\nabla^2\sigma_x = E\varepsilon_x, \tag{38}$$

where e_0a is a material length scale parameter that contains a material constant and internal characteristic length. On the other hand, the resultant axial force and resultant bending moment are ($\hat{N}$ and $\hat{M}$)

$$\hat{N} = \int_{A_0} \sigma_x \mathrm{d}A_0,\ \hat{M} = -\int_{A_0} \sigma_x\,(z - z_0)\,\mathrm{d}A_0. \tag{39}$$

The stress resultants on a beam element can be obtained by substituting Eqs. (35) and (38) into Eq. (39):

$$\hat{N} - (e_0 a)^2\,\nabla^2\hat{N} = \left(\int_{A_0} E\,(z)\,\mathrm{d}A_0\right)\left[\frac{\partial u}{\partial x} + \frac{1}{2}\left(\frac{\partial W}{\partial x}\right)^2\right], \tag{40a}$$

$$\hat{M} - (e_0 a)^2\,\nabla^2\hat{M} = \left(\int_{A_0} (z - z_0)^2\,E\,(z)\,\mathrm{d}A_0\right)\frac{\partial^2 W}{\partial x^2}, \tag{40b}$$

where $E(z)$ and $\rho(z)$ defined by Eq. (41) are the Young's modulus and specific mass density of the FG beam material, respectively.

$$E\,(z) = E_1 + (E_2 - E_1)\left(\frac{2z + h}{2h}\right)^{\overline{n}}, \tag{41a}$$

$$\rho\,(z) = \rho_1 + (\rho_2 - \rho_1)\left(\frac{2z + h}{2h}\right)^{\overline{n}}, \tag{41b}$$

where E_i and ρ_i (i = 1, 2) are the Young's modulus and the specific mass density of the two materials used in the construction of the FG beam, respectively.

The partial differential equation of the transverse motion of FG nanobeams can be derived by combining Eq. (40b) and Eq. (34) and making some simplifications:

$$(e_0 a)^2\,H + \hat{N}\frac{\partial^2 W}{\partial x^2} - \overline{k}W - \overline{c}\frac{\partial W}{\partial t} + F\,(x,t) = \left(\int_{A_0} (z - z_0)^2\,E\,(z)\,\mathrm{d}A_0\right)\frac{\partial^4 W}{\partial x^4} + \left(\int_{A_0} \rho\,(z)\,\mathrm{d}A_0\right)\frac{\partial^2 W}{\partial t^2}, \tag{42}$$

where H is defined by Eq. (43):

$$H = \overline{c}\frac{\partial^3 W}{\partial x^2 \partial t} + \overline{k}\frac{\partial^2 W}{\partial x^2} - \frac{\partial^2 F}{\partial x^2} - \hat{N}\frac{\partial^4 W}{\partial x^4} + \left(\int_{A_0} \rho\,(z)\,\mathrm{d}A_0\right)\frac{\partial^4 W}{\partial x^2 \partial t^2}. \tag{43}$$

On the basis of Eq. (33), one can conclude that $\nabla^2 \hat{N}$ is zero. Therefore, Eq. (40a) is simplified to the relationship between the axial force $\hat{N}$ and displacement components of the midplane of the FG beam (W and u_0) as follows [19,21]:

$$\hat{N} = \left(\int_{A_0} E(z)\, \mathrm{d}A_0 \right) \left[\frac{\partial u_0}{\partial x} + \frac{1}{2} \left(\frac{\partial W}{\partial x} \right)^2 \right]. \tag{44a}$$

Integrating Eq. (44a) yields [19,21]

$$\int_0^L \hat{N} \mathrm{d}x = \int_0^L \left(\left(\int_{A_0} E(z)\, \mathrm{d}A_0 \right) \left[\frac{\partial u_0}{\partial x} + \frac{1}{2} \left(\frac{\partial W}{\partial x} \right)^2 \right] \right) \mathrm{d}x \tag{45a}$$

or

$$\hat{N} L = \left(\int_{A_0} E(z)\, \mathrm{d}A_0 \right) \left[u_0(L) - u_0(0) + \int_0^L \frac{1}{2} \left(\frac{\partial W}{\partial x} \right)^2 \mathrm{d}x \right]. \tag{45b}$$

The boundary values of the axial displacement of nanobeams are [19,21]

$$u_0(0) = 0, \quad u_0(L) = 0. \tag{46}$$

The relationship between the axial force $\hat{N}$ and the transverse displacement of the midplane of nanobeams can be obtained by substituting for boundary conditions from Eq. (46) into Eq. (45b):

$$\hat{N} = +\frac{1}{2L} \left(\int_{A_0} E(z) \mathrm{d}A_0 \right) \int_0^L \left(\frac{\partial W}{\partial x} \right)^2 \mathrm{d}x. \tag{47}$$

Substituting the $\hat{N}$ from Eq. (47) into Eqs. (42) and (43), one can obtain the governing equation of the nonlinear forced lateral vibration of FG nanobeams as follows:

$$(e_0 a)^2 H + \hat{N} \frac{\partial^2 W}{\partial x^2} - \bar{k} W - \bar{c} \frac{\partial W}{\partial t} + F(x,t) = \left(\int_{A_0} (z - z_0)^2 E(z)\, \mathrm{d}A_0 \right) \frac{\partial^4 W}{\partial x^4} + \left(\int_{A_0} \rho(z)\, \mathrm{d}A_0 \right) \frac{\partial^2 W}{\partial t^2}, \tag{48}$$

where H is defined by Eq. (49):

$$H = \bar{c} \frac{\partial^3 W}{\partial x^2 \partial t} + \bar{k} \frac{\partial^2 W}{\partial x^2} - \frac{\partial^2 F}{\partial x^2} - \hat{N} \frac{\partial^4 W}{\partial x^4} + \left(\int_{A_0} \rho(z)\, \mathrm{d}A_0 \right) \frac{\partial^4 W}{\partial x^2 \partial t^2}, \tag{49}$$

and $\hat{N}$ is

$$\hat{N} = +\frac{1}{2L} \left(\int_{A_0} E(z) \mathrm{d}A_0 \right) \int_0^L \left(\frac{\partial W}{\partial x} \right)^2 \mathrm{d}x. \tag{50}$$

The following dimensionless variables are used to simplify the parametric studies:

$$\bar{x} = \frac{x}{L}, \quad \overline{W} = \frac{W}{r}, \quad \bar{t} = t \sqrt{D/\rho_e L^4},$$

$$D = b \int_{-\frac{h}{2}}^{\frac{h}{2}} (z - z_0)^2 E(z)\, \mathrm{d}z, \; \rho_e = b \int_{-\frac{h}{2}}^{\frac{h}{2}} \rho(z)\, \mathrm{d}z, \; A = b \int_{-\frac{h}{2}}^{\frac{h}{2}} E(z)\, \mathrm{d}z, \; r = \sqrt{bh^3/12(bh)}. \tag{51}$$

Then, the governing partial deferential equation of motion changes to

$$-\frac{L^4\,(e_0a)^2}{rD}\overline{H}+\frac{\partial^2\overline{W}}{\partial\overline{t}^2}+\frac{\partial^4\overline{W}}{\partial\overline{x}^4}+\frac{\overline{k}L^4}{D}\overline{W}+\frac{\overline{c}L^2}{\sqrt{D\rho_e}}\frac{\partial\overline{W}}{\partial\overline{t}}-\left(\frac{Ar^2}{2D}\int_0^1\left(\frac{\partial\overline{W}}{\partial\overline{x}}\right)^2\mathrm{d}\overline{x}\right)\frac{\partial^2\overline{W}}{\partial\overline{x}^2}=F\frac{L^4}{rD}, \tag{52}$$

where

$$\overline{H}=-\frac{1}{L^2}\frac{\partial^2F}{\partial\overline{x}^2}+\frac{\overline{k}r}{L^2}\frac{\partial^2\overline{W}}{\partial\overline{x}^2}+\frac{\overline{c}r}{L^2}\sqrt{\frac{D}{\rho_eL^4}}-\left[\frac{Ar^3}{2L^6}\int_0^1\left(\frac{\partial\overline{W}}{\partial\overline{x}}\right)^2\mathrm{d}\overline{x}\right]\frac{\partial^4\overline{W}}{\partial\overline{x}^4}+\frac{Dr}{L^6}\frac{\partial^4\overline{W}}{\partial\overline{x}^2\partial\overline{t}^2}. \tag{53}$$

Appendix 2

According to Eq. (10), it can be found that the secular terms are eliminated from q_{11}, q_{k1}, and $q_{n1}(n\neq1,k)$ if

$$2i\overline{\omega}_1\left(A_1'+\hat{C}_1A_1\right)+2a_1A_1\sum_{m=1}^{N}m^2\left(A_m\overline{A}_m+\Lambda_m^2\right)+3a_1\overline{A}_1^2\Lambda_1\exp\left(i\sigma T_2\right)+4a_1\Lambda_1^2A_1+a_1\overline{A}_1A_1^2=0, \tag{54}$$

$$\begin{aligned}&2i\overline{\omega}_k\left(A_k'+\hat{C}_kA_k\right)+2a_kA_k\sum_{m=1}^{N}m^2\left(A_m\overline{A}_m+\Lambda_m^2\right)+3a_1\overline{A}_1^2\Lambda_1\exp\left(i\sigma T_2\right)+4a_k k^2\Lambda_k^2A_k+k^2a_k\overline{A}_kA_k^2\\&\quad+3a_k\Lambda_k\exp\left(i\sigma_1T_2\right)\sum_{m=1}^{N}m^2\Lambda_m^2=0,\end{aligned} \tag{55}$$

$$2i\overline{\omega}_n\left(A_n'+\hat{C}_nA_n\right)+2a_nA_n\sum_{m=1}^{N}m^2\left(A_m\overline{A}_m+\Lambda_m^2\right)+4a_nn^2\Lambda_n^2A_n+n^2a_n\overline{A}_nA_n^2=0. \tag{56}$$

Let

$$A_m=\frac{1}{2}\alpha_m\exp(i\beta_m), \tag{57}$$

where $\alpha_m\,(T_2)$ and $\beta_m\,(T_2)$ are both real. Substituting Eq. (57) into Eq. (54), Eq. (55), and Eq. (56) and separating the result into real and imaginary parts, one obtains

$$\alpha_1'+\hat{C}_1\alpha_1+\frac{3}{4}\frac{a_1\Lambda_1\alpha_1^2}{\overline{\omega}_1}\sin\gamma_1=0, \tag{58}$$

$$-\alpha_1\beta_1'+a_1\alpha_1\sum_{m=2}^{N}m^2\left(\frac{\alpha_m^2}{4}+\Lambda_m^2\right)+\frac{3}{4}a_1\alpha_1^2\Lambda_1\cos\left(\sigma T_2-3\beta_1\right)+3a_1\Lambda_1^2\alpha_1+\frac{3}{8}a_1\alpha_1^3=0, \tag{59}$$

$$\alpha_k'\overline{\omega}_k+\hat{C}_k\alpha_k\overline{\omega}_k+3a_k\Lambda_k\sum_{m=1}^{N}m^2\Lambda_m^2\sin\gamma_2=0, \tag{60}$$

$$-\alpha_k\beta_k'\overline{\omega}_k+3a_k\Lambda_k\sum_{m=1}^{N}m^2\Lambda_m^2\cos\gamma_2+a_k\alpha_k\sum_{m=1}^{N}m^2\left(\frac{\alpha_m^2}{4}+\Lambda_m\right)+2k^2a_k\Lambda_k^2\alpha_k+\frac{k^2}{8}a_k\alpha_k^3=0, \tag{61}$$

$$\overline{\omega}_n\left(\alpha_n'+\hat{C}_n\alpha_n\right)=0, \tag{62}$$

$$-\overline{\omega}_n\alpha_n\beta_n'+a_n\alpha_n\sum_{m=1}^{N}\frac{m^2}{4}\left(\alpha_m^2+4\Lambda_m^2\right)+2a_nn^2\Lambda_n^2\alpha_n+\frac{1}{8}n^2a_n\alpha_n^3=0, \tag{63}$$

where $\sigma T_2-3\beta_1=\gamma_1$, $\sigma_1T_2-\beta_k=\gamma_2$, and $()'=d/dT_2$.

The solution of Eq. (62) shows that

$$\alpha_n \propto \exp(-\hat{C}_n T_2). \tag{64}$$

Equation (64) clearly reveals that all $\alpha_n (n \neq 1, k)$ decay. Hence, the steady-state motion ($\alpha_1' = 0, \alpha_k' = 0, \gamma_1' = 0, \gamma_k' = 0$) can be expressed as

$$\hat{C}_1 \alpha_1 \overline{\omega}_1 + \frac{3}{4} a_1 \Lambda_1 \alpha_1^2 \sin \gamma_1 = 0, \tag{65}$$

$$-\frac{1}{3}\sigma \alpha_1 \overline{\omega}_1 + a_1 \alpha_1 \sum_{m=2}^{N} m^2 \Lambda_m^2 + \frac{3}{4} a_1 \alpha_1^2 \Lambda_1 \cos(\gamma_1) + \frac{k^2}{4} \alpha_1 a_1 \alpha_k^2 + 3 a_1 \Lambda_1^2 \alpha_1 + \frac{3}{8} a_1 \alpha_1^3 = 0, \tag{66}$$

$$\hat{C}_k \alpha_k \overline{\omega}_k + a_k \Lambda_k \sum_{m=1}^{N} m^2 \Lambda_m^2 \sin \gamma_2 = 0, \tag{67}$$

$$-\alpha_k \sigma_1 \overline{\omega}_k + a_k \Lambda_k \sum_{m=1}^{N} m^2 \Lambda_m^2 \cos \gamma_2 + \frac{3}{8} a_k k^2 \alpha_k^3 + \frac{1}{4} a_k \alpha_k \alpha_1^2 + a_k \alpha_k \sum_{m=1}^{N} m^2 \Lambda_m^2 + 2k^2 a_k \Lambda_k^2 \alpha_k = 0. \tag{68}$$

Combining Eq. (65) with Eq. (66) leads to

$$\left(\frac{3}{4} a_1 \Lambda_1 \alpha_1^2\right)^2 = \left(-\frac{1}{3}\sigma \alpha_1 \overline{\omega}_1 + a_1 \alpha_1 \sum_{m=2}^{N} m^2 \Lambda_m^2 + \frac{k^2}{4} \alpha_1 a_1 \alpha_k^2 + 3 a_1 \Lambda_1^2 \alpha_1 + \frac{3}{8} a_1 \alpha_1^3\right)^2 + \left(\hat{C}_1 \alpha_1 \overline{\omega}_1\right)^2. \tag{69}$$

Eliminating γ_2 from Eq. (67) and Eq. (68) yields

$$\left(a_k \Lambda_k \sum_{m=1}^{N} m^2 \Lambda_m^2\right)^2 = \left(-\alpha_k \sigma_1 \overline{\omega}_k + \frac{3}{8} a_k k^2 \alpha_k^3 + \frac{1}{4} a_k \alpha_k \alpha_1^2 + a_k \alpha_k \sum_{m=1}^{N} m^2 \Lambda_m^2 + 2k^2 a_k \Lambda_k^2 \alpha_k\right)^2 + \left(\hat{C}_k \alpha_k \overline{\omega}_k\right)^2. \tag{70}$$

According to Eqs. (69) and (70), these two solutions are possible: either $\alpha_1 = 0$ and $\alpha_k \neq 0$ or $\alpha_1 \neq 0$ and $\alpha_k \neq 0$.

The following equation expresses the time-dependent lateral deflection of a vibrating FG nanobeam:

$$\begin{aligned} \overline{W}(\overline{x}, \overline{t}) = {} & \varepsilon \alpha_1 \cos\left(\frac{1}{3}\overline{\Omega t} - \frac{1}{3}\gamma_1\right) \sin(\pi \overline{x}) + \varepsilon \alpha_k \cos\left(3\overline{\Omega t} - \gamma_2\right) \sin(k\pi \overline{x}) \\ & + 2\varepsilon \sum_{n=1}^{N} \Lambda_n \cos\left(\overline{\Omega t}\right) \sin(n\pi \overline{x}) + O\left(\varepsilon^3\right). \end{aligned} \tag{71}$$

Appendix 3

It can be found that Eqs. (58)–(63) govern the conditions in which secular terms are eliminated from q_{11}, q_{k1} and $q_{n1} (n \neq 1, k, p, q)$.

The following equations must be satisfied to eliminate the secular terms from q_{p1} and q_{q1}:

$$\begin{aligned} & 2i\overline{\omega}_p \left(A_p' + \hat{C}_p A_p\right) + 2a_p A_p \sum_{m=1}^{N} m^2 \left(A_m \overline{A}_m + \Lambda_m^2\right) + 4a_p p^2 \Lambda_p^2 A_p + p^2 a_p \overline{A}_p A_p^2 \\ & + 2a_p \Lambda_q \Lambda_p \overline{A}_q \exp(\sigma_2 T_2) = 0, \end{aligned} \tag{72}$$

$$\begin{aligned} & 2i\overline{\omega}_q \left(A_q' + \hat{C}_q A_q\right) + 2a_q A_q \sum_{m=1}^{N} m^2 \left(A_m \overline{A}_m + \Lambda_m^2\right) + 4a_q q^2 \Lambda_q^2 A_q + q^2 a_q \overline{A}_q A_q^2 \\ & + 2a_q \Lambda_q \Lambda_p \overline{A}_p \exp(\sigma_2 T_2) = 0. \end{aligned} \tag{73}$$

The following equations can be found by introducing the polar notation represented by Eq. (57):

$$\overline{\omega}_p\left(\alpha_p' + \hat{C}_p\alpha_p\right) + a_p\Lambda_p\Lambda_q\alpha_q\sin(\gamma_3) = 0, \tag{74}$$

$$-\overline{\omega}_p\alpha_p\beta_p' + a_p\alpha_p\sum_{m=1}^{N}\frac{m^2}{4}\left(\alpha_m^2 + 4\Lambda_m^2\right) + 2a_pp^2\Lambda_p^2\alpha_p + \frac{1}{8}p^2a_p\alpha_p^3 + a_p\Lambda_p\Lambda_q\alpha_q\cos(\gamma_3) = 0, \tag{75}$$

$$\overline{\omega}_q\left(\alpha_q' + \hat{C}_q\alpha_q\right) + a_q\Lambda_q\Lambda_p\alpha_p\sin(\gamma_3) = 0, \tag{76}$$

$$-\overline{\omega}_q\alpha_q\beta_q' + a_q\alpha_q\sum_{m=1}^{N}\frac{m^2}{4}\left(\alpha_m^2 + 4\Lambda_m^2\right) + 2a_qq^2\Lambda_q^2\alpha_q + \frac{1}{8}q^2a_q\alpha_q^3 + a_q\Lambda_q\Lambda_p\alpha_p\cos(\gamma_3) = 0, \tag{77}$$

in which $\gamma_3 = \sigma_2T_2 - \beta_p - \beta_q$.

As mentioned earlier, except for α_1, α_k, α_p and α_q, the remaining α_n ($n \neq 1, k, p, q$) decay with time. Thus, the following equations govern the steady-state response of FG nanobeams:

$$\overline{\omega}_p\hat{C}_p\alpha_p + a_p\Lambda_p\Lambda_q\alpha_q\sin(\gamma_3) = 0, \tag{78}$$

$$\overline{\omega}_q\hat{C}_q\alpha_q + a_q\Lambda_q\Lambda_p\alpha_p\sin(\gamma_3) = 0, \tag{79}$$

$$\sigma_2 = \beta_p' + \beta_q', \tag{80}$$

$$\begin{aligned}\beta_p' = {} & \frac{1}{\overline{\omega}_p\alpha_p}\left(a_p\alpha_p\sum_{m=1}^{N}m^2\Lambda_m^2\frac{m^2}{4} + \frac{q^2}{4}a_p\alpha_p\alpha_q^2 + \frac{1}{4}a_p\alpha_p\alpha_1^2 + \frac{k^2}{4}a_p\alpha_p\alpha_k^2 + 2a_pp^2\Lambda_p^2\alpha_p\right)\\ & + \frac{1}{\overline{\omega}_p\alpha_p}\left(\frac{3}{8}p^2a_p\alpha_p^3 + a_p\Lambda_p\Lambda_q\alpha_q\cos(\gamma_3)\right),\end{aligned} \tag{81}$$

$$\begin{aligned}\beta_q' = {} & \frac{1}{\overline{\omega}_q\alpha_q}\left(a_q\alpha_q\sum_{m=1}^{N}m^2\Lambda_m^2\frac{m^2}{4} + \frac{p^2}{4}a_q\alpha_q\alpha_p^2 + \frac{1}{4}a_q\alpha_q\alpha_1^2 + \frac{k^2}{4}a_q\alpha_q\alpha_k^2 + 2q^2a_q\Lambda_q^2\alpha_q\right)\\ & + \frac{1}{\overline{\omega}_q\alpha_q}\left(\frac{3}{8}q^2a_q\alpha_q^3 + a_q\Lambda_q\Lambda_p\alpha_p\cos(\gamma_3)\right),\end{aligned} \tag{82}$$

$$\hat{C}_1\alpha_1\overline{\omega}_1 + \frac{3}{4}a_1\Lambda_1\alpha_1^2\sin\gamma_1 = 0, \tag{83}$$

$$\begin{aligned}& -\frac{1}{3}\sigma\alpha_1\overline{\omega}_1 + a_1\alpha_1\sum_{m=2}^{N}m^2\Lambda_m^2 + \frac{3}{4}a_1\alpha_1^2\Lambda_1\cos(\gamma_1) + \frac{k^2}{4}\alpha_1a_1\alpha_k^2 + 3a_1\Lambda_1^2\alpha_1 + \frac{3}{8}a_1\alpha_1^3\\ & + \frac{3}{4}p^2\alpha_1a_1\alpha_p^2 + \frac{3}{4}q^2\alpha_1a_1\alpha_q^2 = 0,\end{aligned} \tag{84}$$

$$\hat{C}_k\alpha_k\overline{\omega}_k + a_k\Lambda_k\sum_{m=1}^{N}m^2\Lambda_m^2\sin\gamma_2 = 0, \tag{85}$$

$$\begin{aligned}& -\alpha_k\sigma_1\overline{\omega}_k + a_k\Lambda_k\sum_{m=1}^{N}m^2\Lambda_m^2\cos\gamma_2 + \frac{3}{8}a_kk^2\alpha_k^3 + \frac{1}{4}a_k\alpha_k\alpha_1^2 + a_k\alpha_k\sum_{m=1}^{N}m^2\Lambda_m^2 + 2k^2a_k\Lambda_k^2\alpha_k\\ & + \frac{p^2}{4}\alpha_ka_k\alpha_p^2 + \frac{q^2}{4}\alpha_ka_k\alpha_q^2 = 0.\end{aligned} \tag{86}$$

According to Eqs. (78), (79), and (83), the possible solutions are

(a) $\alpha_1 = \alpha_p = \alpha_q = 0$, and $\alpha_k \neq 0$.
(b) $\alpha_1 \neq 0$, and $\alpha_k \neq 0$, but $\alpha_p = \alpha_q = 0$.
(c) $\alpha_1 = 0$, and $\alpha_k \neq 0$, $\alpha_p \neq 0$, and $\alpha_q \neq 0$.

(d) $\alpha_1 \neq 0$, $\alpha_k \neq 0$,$\alpha_p \neq 0$, and $\alpha_q \neq 0$.

The lateral deflection of vibrating FG nanobeams can be represented by the following equation:

$$\overline{W}\left(\overline{x},\overline{t}\right) = \varepsilon\alpha_1 \cos\left(\frac{1}{3}\overline{\Omega}\overline{t} - \frac{1}{3}\gamma_1\right)\sin\left(\pi\overline{x}\right) + \varepsilon\alpha_k \cos\left(3\overline{\Omega}\overline{t} - \gamma_2\right)\sin\left(k\pi\overline{x}\right) + \varepsilon\alpha_p \cos\left(\overline{\omega}_p\overline{t} + \beta_P\right)\sin\left(p\pi\overline{x}\right)$$
$$+ \varepsilon\alpha_q \cos\left(\overline{\omega}_q\overline{t} + \beta_q\right)\sin\left(q\pi\overline{x}\right) + 2\varepsilon\sum_{n=1}^{N}\Lambda_n \cos\left(\overline{\Omega}\overline{t}\right)\sin\left(n\pi\overline{x}\right) + O\left(\varepsilon^3\right). \quad (87)$$

References

1. Ke L-L, Yang J, Kitipornchai S, Bradford MA (2012) Bending, buckling and vibration of size-dependent functionally graded annular microplates. Compos Struct 94:3250–3257
2. Kanani AS, Niknam H, Ohadi AR, Aghdam MM (2014) Effect of nonlinear elastic foundation on large amplitude free and forced vibration of functionally graded beam. Compos Struct 115:60–68
3. Simsek M, Yurtcu HH (2013) Analytical solutions for bending and buckling of functionally graded nano-beams based on the nonlocal Timoshenko beam theory. Compos Struct 97:378–386
4. Lei J, He Y, Zhang B, Gan Z, Zeng P (2013) Bending and vibration of functionally graded sinusoidal microbeams based on the strain gradient elasticity theory. Int J Eng Sci 72:36–52
5. Askes H, Aifantis EC (2011) Gradient elasticity in statics and dynamics: an overview of formulations, length scale identification procedures, finite element implementations and new results. Int J Solids Struct 48:1962–1990
6. Ansari R, Gholami R, Sahmani S (2011) Free vibration analysis of size-dependent functionally graded microbeams based on the strain gradient Timoshenko beam theory. Compos Struct 94:221–228
7. Ansari R, Gholami R, FaghihShojaei M, Mohammadi V, Sahmani S (2013) Size-dependent bending, buckling and free vibration of functionally graded Timoshenko microbeams based on the most general strain gradient theory. Compos Struct 100:385–397
8. Setoodeh AR, Afrahim S (2014) Nonlinear dynamic analysis of FG micro-pipes conveying fluid based on strain gradient theory. Compos Struct 116:128–135
9. Reddy JN (2011) Microstructure-dependent couple stress theories of functionally graded beams. J Mech Phys Solids 59(9):2382–2399
10. Arbind A, Reddy JN (2013) Nonlinear analysis of functionally graded microstructure-dependent beams. Compos Struct 98:272–281
11. Eltaher MA, Khairy A, Sadoun AM, Omar F-A (2014) Static and buckling analysis of functionally graded Timoshenko nanobeams. Appl Math Comput 229:283–295
12. Eltaher MA, Emam SA, Mahmoud FF (2013) Static and stability analysis of nonlocal functionally graded nanobeams. Compos Struct 96:82–88
13. Eltaher MA, Emam SA, Mahmoud FF (2012) Free vibration analysis functionally graded size-dependent nano-beams. Appl Math Comput 218:7406–7420
14. Eltaher MA, Alshorbagy AE, Mahmoud FF (2013) Determination of neutral axis position and its effect on natural frequencies of functionally graded macro/nano-beams. Compos Struct 99:193–201
15. Eltaher MA, Abdelrahman AA, Al-Nabawy A, Khater M, Mansour A (2014) Vibration of nonlinear graduation of nano-Timoshenko beam considering the neutral axis position. Appl Math Comput 235:512–529
16. Rahmani O, Pedram O (2014) Analysis and modeling the size effect on vibration of functionally graded nano-beams based on nonlocal Timoshenko beam theory. Int J Eng Sci 77:55–70
17. Ebrahimi F, Salari E (2015) Size-dependent free flexural vibrational behavior of functionally graded nanobeams using semi-analytical differential transform method. Composites B 79:156–169
18. Uymaz B (2013) Forced vibration analysis of functionally graded beams using nonlocal elasticity. Compos Struct 105:227–239
19. Nazemnezhad R, Hosseini-Hashemi Sh (2014) Nonlocal nonlinear free vibration of functionally graded nano-beams. Compos Struct 110:192–199
20. Niknam H, Aghdam MM (2015) A semi analytical approach for large amplitude free vibration and buckling of nonlocal FG beams resting on elastic foundation. Compos Struct 119:452–462
21. Ziaee S (2015) Small scale effect on linear vibration of buckled size-dependent FG nanobeam. Ain Shams Eng J 6:587–598
22. Ebrahimi F, Salari E (2015) Thermal buckling and free vibration analysis of size dependent Timoshenko FG nanobeams in thermal environments. Compos Struct 128:363–380
23. Ebrahimi F, Salari E (2015) Thermo-mechanical vibration analysis of nonlocal temperature-dependent FG nanobeams with various boundary conditions. Composites B 78:272–290
24. Ebrahimi F, Salari E (2015) Nonlocal thermo-mechanical vibration analysis of functionally graded nanobeams in thermal environment. Acta Astron 113:29–50
25. Zhang YQ, Liu GR, Xie XY (2005) Free transverse vibrations of double-walled carbon nanotubes using a theory of nonlocal elasticity. Phys Rev B 9:195404

26. Hu Y-G, Liew KM, Wang Q, He XQ, Yakobson BI (2008) Nonlocal shell model for elastic wave propagation in single- and doublewalled carbon nanotubes. J Mech Phys Solids 56:3475–3485
27. Khademolhosseini F, Rajapakse RKND, Nojeh A (2010) Torsional buckling of carbon nanotubes based on nonlocal elasticity shell models. Compos Mater Sci 48:736–742
28. Ansari R, Sahmani S, Rouhi H (2011) Rayleigh-Ritz axial buckling analysis of single-walled carbon nanotubes with different boundary conditions. Phys Lett A 375:1255–1263
29. Duan WH, Wang CM, Zhang YY (2007) Calibration of nonlocal scaling effect parameter for free vibration of carbon nanotubes by molecular dynamics. J Appl Phys 101:024305
30. Ansari R, Sahmani S, Arash B (2010) Nonlocal plate model for free vibrations of single-layered graphene sheets. Phys Lett A 375:53–62
31. Shen L, Shen H-S, Zhang C-L (2010) Anonlocal plate model for nonlinear vibration of single layer graphene sheets in thermal environments. Comput Mater Sci 48:680–685
32. Ansari R, Sahmani S (2013) Prediction of biaxial buckling of single-layered graphene sheets based on nonlocal plate models and molecular dynamics simulations. Appl Math Model 37:7338–7351
33. Miandoab EM, Pishkenari HN, Yousefi-Koma A, Hoorzad H (2014) Polysiliconnano-beam model based on modified couple stress and Eringen'snonlocal elasticity theories. Physica E 63:223–228
34. Peddieson J, Buchanan GR, McNitt RP (2003) Application of nonlocal continuum models to nanotechnology. Int J Eng Sci 41:305–312
35. Shen H-S, Xu Y-M, Zhang C-L (2013) Prediction of nonlinear vibration of bilayer graphene sheets in thermal environments via molecular dynamics simulations and nonlocal elasticity. Comput Method Appl Mech Eng 267:458–470
36. Yang J, Ke LL, Kitipornchai S (2010) Nonlinear free vibration of single-walled carbon nanotubes using nonlocal Timoshenko beam theory. Phys E 42:1727–1735
37. Ke LL, Xiang Y, Yang J, Kitipornchai S (2009) Nonlinear free vibration of embedded double-walled carbon nanotubes based on nonlocal Timoshenko beam theory. Comput Mater Sci 47:409–417
38. Karaoglu P, Aydogdu M (2010) On the forced vibration of carbon nanotubes via a non-local Euler–Bernoulli beam model. J Mech Eng Sci 224(2):497–503
39. Sudak LJ (2003) Column buckling of multiwalled carbon nanotubes using nonlocal continuum mechanics. J Appl Phys 9:7281
40. Aydogdu M (2009) A general nonlocal beam theory: Its application to nanobeam bending, buckling and vibration. Physica E 41:1651–1655
41. Nayfeh AH, Emam SA (2008) Exact solution and stability of postbuckling configurations of beams. Nonlinear Dyn 54:395–408
42. Nayfeh AH, Mook DT (1995) Nonlinear oscillations. Wiley, New York